CHROM. 7714

RECENT PROGRESS IN THE FIELD OF SYNTHETIC INORGANIC EXCHANGERS HAVING A LAYERED OR FIBROUS STRUCTURE

GIULIO ALBERTI and UMBERTO COSTANTINO

Istituto di Chimica Inorganica, Università di Perugia, Via Elce di Sotto, Perugia (Italy)

SUMMARY

In the first part, recent results on crystalline insoluble acid salts of tetravalent metals having a layered structure are critically examined. The dependence of the interlayer distance of crystalline zirconium phosphate on its water content and counter ions is discussed and an ion-exchange mechanism for monovalent and divalent ions, in both aqueous and molten salt media, is proposed. Furthermore, the effect of the degree of crystallinity of zirconium phosphate on its ion-exchange properties and electrical conductivity, the dependence of its selectivity for large cations on steric hindrance and the catalytic effect of small amounts of sodium ions on the exchange of large hydrated cations are also discussed. Other layered exchangers, such as zirconium arsenate and titanium phosphate, are also considered and some general points on their ion-exchange properties as a function of the tetravalent metal ion and polybasic acid groups involved are made.

The second part deals with the synthesis and ion-exchange properties of fibrous inorganic ion exchangers with special regard to fibrous cerium(IV) phosphate.

In the third part, some practical applications of the exchangers examined, in both ion-exchange and electrochemical processes, are reported.

INTRODUCTION

Ion exchange is now a well established technique in many industrial processes and is also widely employed in many chemical laboratories. However, the applications of ion exchange to some important processes that occur at high temperatures or in the presence of ionizing radiation or highly oxidizing media are severely limited at present, because commercially available ion-exchange resins undergo degradation under such drastic conditions.

The revived interest in inorganic ion exchangers is due primarily to their high resistance towards temperature and radiation, so that several new potential applications of ion-exchange technology can be expected.

A large number of new synthetic inorganic exchangers has been obtained and their ion-exchange properties investigated. Several of these exchangers were found to exhibit the expected chemical stability and sometimes they proved to be highly selective for certain ions.

These exchangers can conveniently be divided into the following principal groups:

(1) Insoluble acid salts of polyvalent metals.

(2) Hydrous oxides of polyvalent metals.

(3) Salts of heteropolyacids.

(4) Insoluble hexacyanoferrates(II).

(5) Synthetic aluminosilicates.

(6) Miscellaneous inorganic exchangers, e.g., mercabide salts and potassium polyphosphate.

In the present paper, we are concerned exclusively with inorganic exchangers of the first group. Concerning the exchangers of the other groups, the interested reader is referred to recent reviews by Vesely and Pekárek[1,2].

Until recently, the insoluble acid salts of polyvalent metals have been obtained as gels with no definite composition and not very stable towards hydrolysis of their acid groups. Some of these compounds, particularly the amorphous zirconium phosphate, exhibit a high selectivity for some important cations such as Cs^+ and UO_2^{2+} and therefore extensive studies have been carried out on these exchangers. The ion-exchange properties of amorphous exchangers were reviewed in 1964 by Amphlett[3]. New developments in this field led to the synthesis of several exchangers having a fixed composition and a well defined crystalline structure[4-22].

These crystalline exchangers can be divided into the following three sub-groups:

(a) Exchangers having a layered structure.

(b) Exchangers having a fibrous structure.

(c) Exchangers having an as yet unknown structure.

We will consider here in detail only the insoluble acid salts of tetravalent metals having a layered or a fibrous structure, while some exchangers of sub-group (c) are briefly discussed only in connection with their practical applications. Additional information can be found in a recent review by Clearfield et al.[23].

EXCHANGERS HAVING A LAYERED STRUCTURE

Introduction

Some important exchangers of this sub-group are listed in Table I. Among these exchangers, crystalline zirconium phosphate is certainly the most widely investigated and therefore we shall consider in detail only this exchanger, while the remaining exchangers are briefly discussed with particular regard to their differences from crystalline zirconium phosphate.

TABLE I

INORGANIC ION EXCHANGERS HAVING A LAYERED STRUCTURE

Formula	Ion-exchange capacity (mequiv./g)	Interlayer distance d (Å)	References
$Zr(HPO_4)_2 \cdot H_2O$	6.64	7.56	24
$Ti(HPO_4)_2 \cdot H_2O$	7.76	7.56	5, 6
$Zr(HAsO_4)_2 \cdot H_2O$	5.14	7.82	8, 11, 25
$Ti(HAsO_4)_2 \cdot H_2O$	5.78	7.77	12

Synthesis of crystalline zirconium phosphate

The synthesis of crystalline zirconium phosphate is very important, as recent investigations have revealed that its ion-exchange properties depend on its degree of crystallinity, which, in turn, depends on the method of preparation used[26-28]. At present, there are two main methods of preparation. In the first method, crystalline zirconium phosphate is obtained by refluxing the amorphous product in concentrated phosphoric acid[4]. It was recently found by Alberti *et al.*[29] and Clearfield *et al.*[30] independently that the degree of crystallinity of the exchanger increases with the refluxing time and completely crystalline materials can be obtained only after about 20 days in 12–14 M orthophosphoric acid.

Until recently, most investigations on the ion exchange of crystalline zirconium phosphate have been carried out using materials prepared by refluxing for only 24–100 h in 10–12 M orthophosphoric acid, and which are therefore not completely crystalline; hence some of the results previously obtained must now be treated with caution. In some instances, there is a need to repeat some experiments using completely crystalline material, especially when the ion-exchange behaviour cannot be easily explained on the basis of a regular crystalline structure.

In the second method, first used by Alberti and Torracca[9], zirconium is first complexed with hydrofluoric acid and then the fluoro-complex is slowly decomposed (*e.g.*, by decreasing the hydrofluoric acid concentration in solution) in the presence of orthophosphoric acid until crystalline zirconium phosphate starts to precipitate. By slowly evaporating the hydrofluoric acid at room temperature, large crystals, suitable for column applications, can be obtained, but the precipitation requires a long time. However, the decomposition rate of the zirconium fluoro-complex can be accelerated by warming the solution at *ca.* 80° and/or passing through it a stream of nitrogen; in order to avoid water evaporation, the nitrogen is pre-humidified by bubbling it through boiling water. Rapid precipitation is completed in about 4 days with a yield of *ca.* 80 % and it still provides crystals larger than those obtained by the refluxing procedure[29,31]. It was first found by Alberti *et al.*[29] and then confirmed by Horsley and Nowell[32] that the direct precipitation method gives zirconium phosphate with high degree of crystallinity even when it is obtained by rapid precipitation. Thus, when crystalline zirconium phosphate with a high degree of crystallinity is required, precipitation in the presence of hydrofluoric acid is a more rapid method than the refluxing method (*ca.* 4 days compared with *ca.* 20 days); therefore, we are now almost exclusively using crystalline zirconium phosphate prepared according to the precipitation method in the presence of hydrofluoric acid.

Structural data for crystalline zirconium phosphate

The hydrogen form has been shown to be zirconium bis(monohydrogen orthophosphate), $Zr(HPO_4)_2 \cdot H_2O$, and its crystal structure has recently been established by Clearfield and Smith[24]. This structure, shown schematically in Fig. 1, is a layered one and is similar in many respects to that of clay minerals. Each layer consists of zirconium atoms lying very nearly in a plane and bridged through phosphate groups located above and below this plane; each sandwich of this type can be considered as a giant molecule. The crystal structure of zirconium phosphate $(Zr_n(HPO_4)_{2n} \cdot nH_2O)$ is built up by the bonding together of these sandwiches by long hydrogen bonds or Van der Waals forces. In this arrangement, each phosphorus atom in the lower sand-
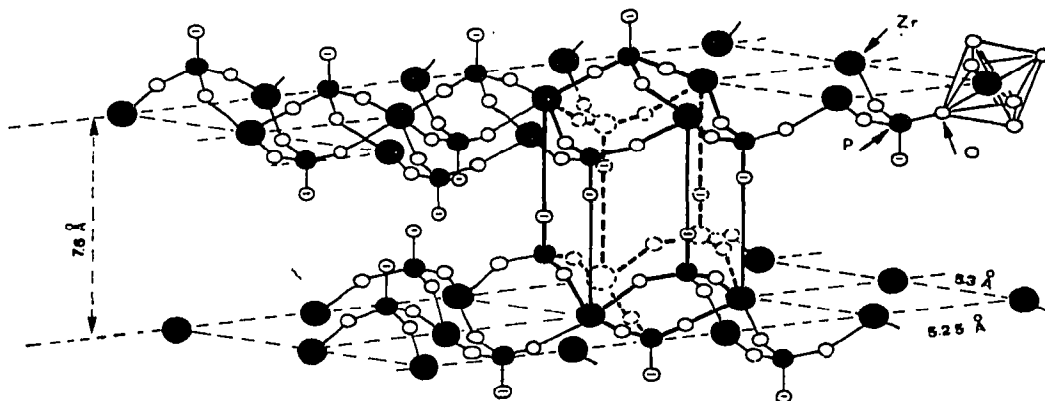
Fig. 1. Idealized crystal structure of zirconium phosphate. Solid lines show one of the zeolitic cavities created by the arrangement of the layers.

wich lies along a perpendicular line drawn from the zirconium atom of the upper sandwich. This arrangement creates zeolitic-type cavities that are interconnected by windows whose maximum diameter, for the hydrogen form, is 2.64 Å. Both hydrogen atoms can be exchanged with other cations so that the total ion-exchange capacity is 6.64 mequiv. of cation per gram of $Zr(HPO_4)_2 \cdot H_2O$.

In the following discussion, for the sake of brevity, the various ionic forms are simply indicated by their counter ions (under a bar) and water content, while their interlayer distances are reported in parentheses. Thus, for example, $Zr(HPO_4)_2 \cdot H_2O$ and $ZrHNa(PO_4)_2 \cdot 5H_2O$ will be written as $\overline{HH} \cdot H_2O$ (7.6 Å) and $\overline{HNa} \cdot 5H_2O$ (11.8 Å).

So far, the reticular position of the counter ions in the salt forms of crystalline zirconium phosphate has been determined only for the NH_4^+ form[25] owing to the difficulties involved in obtaining crystals of other ionic forms of a suitable size for structural determinations. Furthermore, the position of the water molecules in the hydrated salt forms of zirconium phosphate is as yet unknown.

On the other hand, the knowledge of the crystal structure of the various phases obtained in a given ion-exchange process is very important, as it provides the opportunity of relating the observed ion-exchange properties with the local structure. Therefore, research on the crystal structure of various salt forms is particularly necessary. At present, without the knowledge of the crystal structures of the salt forms, one can try to interpret the ion-exchange mechanism from other parameters such as the variation in the interlayer distance and water content in a given ion-exchange process.

Interlayer distance of crystalline zirconium phosphate in various ionic forms with different degrees of hydration

When the hydrogen ion in $\overline{HH} \cdot H_2O$ (7.6 Å) is exchanged with other counter ions, it is likely that the arrangement of zirconium atoms and phosphate groups, in each sandwich, remains about the same; consequently, the crystalline structure of the salt forms of zirconium phosphate will be essentially that of the dihydrogen form, with the layers at new distances in order to accommodate the exchanged counter

ions. Thus the first maximum of the X-ray powder pattern of a given ionic form of crystalline zirconium phosphate provides its interlayer distance. This view is now generally accepted and has recently been confirmed by working out the crystal structure of the $\overline{NH_4NH_4}\cdot H_2O$ (9.36 Å) phase[25].

The interlayer distances of several salt forms of crystalline zirconium phosphate containing two identical monovalent counter ions are given in Table II (column 3). A simple inspection of these values shows that the interlayer distance increases with the water content of the exchanger and that, for the same water content, it increases with increasing crystalline radius of the monovalent counter ion. Furthermore, it can easily be seen that the experimental difference between the interlayer distances of two monohydrated forms, $\overline{MM}\cdot H_2O$ and $\overline{M'M'}\cdot H_2O$, is approximately equal to the dif-

TABLE II

EXPERIMENTAL AND CALCULATED INTERLAYER DISTANCES OF HYDRATED AND ANHYDROUS PHASES OF CRYSTALLINE ZIRCONIUM PHOSPHATE COMPLETELY EXCHANGED WITH THE SAME MONOVALENT ION

Phase composition	Drying conditions*	Interlayer distance, d (Å)	Interlayer distance (calculated value)**, d (Å)	References
$\overline{HH}\cdot 8H_2O$	r.t. ($P/P_0 = 1$)	10.4		21, 16, 20
$\overline{HH}\cdot H_2O$	r.t. over P_4O_{10}	7.56		4
$\overline{HH}$	110°	7.56		4
$\overline{LiLi}\cdot 4H_2O$	r.t. ($P/P_0 = 0.9$)	10.1; 9.98	10.0	33, 34, 35
$\overline{LiLi}\cdot 2H_2O$	r.t. over P_4O_{10}	8.84; 8.80; 8.87	8.8	35, 33, 36, 37
$\overline{LiLi}\cdot H_2O$	100–150°	8.87; 7.89; 7.91	7.9	37, 33, 34
$\overline{LiLi}$	300°	7.05; 7.0		33, 34, 38
$\overline{LiLi}$	400–800°	6.24		33
$\overline{NaNa}\cdot 3H_2O$	r.t. ($P/P_0 = 0.7$)	9.92; 9.83	9.9	34, 39
$\overline{NaNa}\cdot H_2O$	r.t. over P_4O_{10}	8.42	8.4	39, 37
$\overline{NaNa}$	165°	8.38		39
$\overline{NaNa}$	300–400°	7.63; 7.7		39, 38
$\overline{KK}\cdot 3H_2O$	r.t. ($P/P_0 = 0.7$)	10.74; 10.8	10.7	34, 35, 40
$\overline{KK}\cdot H_2O$	r.t. over P_4O_{10}	8.84; 8.90	8.9	40, 35, 36, 37
$\overline{KK}$	110–450°	8.93; 9.0; 9.02		34, 38, 40
$\overline{RbRb}\cdot H_2O$	r.t. ($P/P_0 = 0.9$)	9.20	9.1	31
$\overline{RbRb}$	150°	9.20		31
$\overline{CsCs}\cdot 6H_2O$	r.t. ($P/P_0 = 0.9$)	14.2	13.8	31
$\overline{CsCs}\cdot H_2O$	r.t. over P_4O_{10}	9.5	9.3	31
$\overline{CsCs}$	150°	9.20		31
$\overline{NH_4NH_4}\cdot 2H_2O$		9.02		36
$\overline{NH_4NH_4}\cdot H_2O$		9.36	9.0	25
$\overline{AgAg}\cdot H_2O$	r.t. ($P/P_0 = 0.7$)	8.41	8.8	41

* r.t. = room temperature.
** Calculated by eqn. 1 or 2 using the following values of crystalline ionic radius: Li^+, 0.66 Å; Na^+, 0.97 Å; K^+, 1.33 Å; Rb^+, 1.47 Å; Cs^+, 1.67 Å; Ag^+, 1.26 Å; NH_4^+, 1.43 Å.

ference between the diameters of the two counter ions M and M' (a better agreement is obtained if the difference in diameters is multiplied by a factor of 1.1).

It can also be noted that the interlayer distances of $\overline{KK} \cdot H_2O$ (8.9 Å), $\overline{RbRb} \cdot H_2O$ (9.2 Å) and $\overline{CsCs} \cdot H_2O$ (9.5 Å) phases remain about the same when they lose their water molecule, while there is a slight decrease for $\overline{LiLi} \cdot H_2O$ (7.9 Å) and $\overline{NaNa} \cdot H_2O$ (8.4 Å) phases.

As the interlayer distances of several monohydrated forms do not decrease on dehydration, it can be assumed that the water molecule is situated near the centre of the cavity, where the available space is large enough to accommodate it without causing any change in the interlayer distance of the exchanger. This can easily be seen in Fig. 2, which shows the projection of oxygen atoms, carrying the fixed negative charges, in a plane perpendicular to the crystal axis c and passing in the middle point of the cavity.
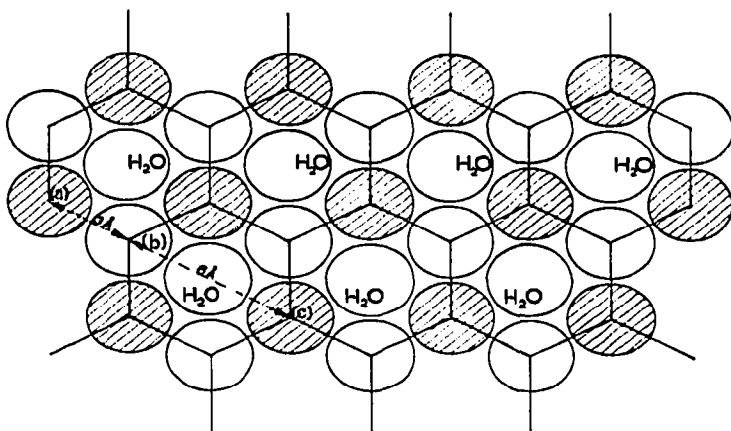

Fig. 2. Arrangement of oxygen atoms, carrying the fixed negative charges, and the water molecules inside the cavities of crystalline zirconium phosphate. The figure shows the projection of these oxygen atoms and water molecules in a plane perpendicular to the crystal axis c and crossing the cavities through their middle points. Hatched circles refer to oxygen atoms lying above the plane while open circles to those lying below the plane.

Thus the monovalent counter ions (two per cavity) should be placed around this water molecule and near two $P-O^-$ groups of the adjacent layers.

By assuming this reticular position for the counter ions and the water molecule, it was possible to show, from geometrical considerations, that the interlayer distance of the monohydrate salt forms of crystalline zirconium phosphate can be calculated as a function of the radius (r) of the counter ion according to the equation[41]

$$d = 2.8 + 3.4 \cos \alpha + (1.4 + r)^2 - 11.56 \sin^2 \alpha \qquad (1)$$

where $\alpha = 46.9 - \text{arcos} (0.95 + 0.1 \, r - 0.036 \, r^2)$.

The calculated values of the interlayer distance are tabulated in column 4 of Table II. It can be seen that the agreement between the experimental and calculated

interlayer distances is very good, which supports our hypothesis about the reticular position of monovalent counter ions and water molecules.

A careful examination of Table II led to the observation that the interlayer distance of hydrated salt forms that have more than one water molecule is higher than that of the corresponding monohydrated phase by 1.8 Å for every two additional water molecules (one for each counter ion). Hence it is very likely that additional water molecules are situated between the counter ion and zirconium atom in order to reduce the electrostatic repulsions and accordingly the approximate interlayer distance, d, of a given salt form can simply be calculated by the relationship

$$d\,(\text{Å}) = \text{interlayer distance of monohydrate form} + (0.9 \times \text{number of additional water molecules}) \qquad (2)$$

where the interlayer distance of the monohydrated form can, in turn, be calculated by the eqn. 1.

In Table III are reported the interlayer distances of several phases of crystalline zirconium phosphate containing two monovalent counter ions of different sizes, at various degrees of hydration. It can be seen that the anhydrous mixed phases $\overline{\text{MM}'}$ (where M' is a larger counter ion than M) have an interlayer distance equal to or slightly higher than that of the pure $\overline{\text{MM}}$ phase. This phenomenon could be explained assuming that, in the mixed salt forms, the larger counter ion is situated further inside the cavity and the smaller one is shifted further towards the sides of the cavity than in the pure salt forms $\overline{\text{M}'\text{M}'}$ and $\overline{\text{MM}}$, respectively, so as to allow only a minimum increase in the interlayer distance. If the two counter ions differ appreciably in their ionic radii, the larger one could even be accommodated near the centre of the cavity while the smaller one could approach a position very near to the side of the cavity. As an example, it can be seen from Table III that the interlayer distances of the anhydrous mixed forms $\overline{\text{HK}}$ (7.5 Å), $\overline{\text{HRb}}$ (7.6 Å) and $\overline{\text{HCs}}$ (7.5 Å) are almost the same and very near to the value of the $\overline{\text{HH}}$ (7.6 Å) form, in agreement with the above assumption. It was further supported from X-ray powder patterns, which show that mixed $\overline{\text{M}_1\text{M}'_1}$ or $\overline{\text{M}_{0.5}\text{M}'_{1.5}}$ phases have a more disordered structure than the pure phases. It can be pointed out that the interlayer distance of hydrated phases containing two different counter ions can also be calculated by eqn. 2 by using a factor of 1.0 instead of 0.9. The reason for this fact, which can be related to the relative positions of water molecules and counter ions, will be discussed elsewhere[41].

Ion-exchange mechanism for zirconium phosphate for monovalent ions

The dependence of the interlayer distance of crystalline zirconium phosphate on water content, and the size of the counter ions involved as well as the shape of the titration curves (or ion-exchange isotherms) and the phase transitions in a given ion-exchange process, enable us to draw the following general conclusions on the ion-exchange mechanism of this exchanger.

Ion exchange in molten salts. Molten salts provide excellent media for investigating ion-exchange processes on zirconium phosphate, because in such media counter ions inside the exchanger are generally unsolvated[48]; thus complications due to count-

TABLE III

INTERLAYER DISTANCES OF HYDRATED AND ANHYDROUS MIXED PHASES OF CRYSTALLINE ZIRCONIUM PHOSPHATE COMPLETELY EXCHANGED WITH TWO DIFFERENT MONOVALENT IONS

Phase composition	Drying conditions[*]	Interlayer distance, $d(\text{Å})$	Ref.	Phase composition	Drying conditions[*]	Interlayer distance, $d(\text{Å})$	Ref.
$\overline{HLi}\cdot 4H_2O$	r.t. $(P/P_0 = 0.9)$	10.1	29	$\overline{H_{1.5}Cs_{0.5}}\cdot 0.5H_2O$	r.t. $(P/P_0 = 0.9)$	7.7	31
$\overline{HLi}$	300°	7.0	42	$\overline{HCs}\cdot 2H_2O$	r.t. $(P/P_0 = 0.9)$	11.3	31
$H_{0.67}Li_{1.33}\cdot 4H_2O$	r.t. $(P/P_0\ 0.6)$	10.0	33	$\overline{HCs}\cdot 0.5H_2O$	r.t. over P_4O_{10}	8.03	31
$H_{0.67}Li_{1.33}\cdot 3.3H_2O$	r.t. over P_4O_{10}	8.55	33	$\overline{HCs}$	150°	7.52	31
$H_{.67}Li_{1.33}\cdot 1.3H_2O$	80°	7.30	33	$H_{0.5}Cs_{1.5}\cdot 3H_2O$	r.t. $(P/P_0 = 0.9)$	11.7	31
$H_{0.67}Li_{1.33}\cdot 0.7H_2O$	130°	7.84	33				
$H_{0.67}Li_{1.33}$	400°	7.00	33	$\overline{HNH_4}$		9.4	37
$H_{0.3}Li_{1.5}\cdot 4H_2O$	r.t. $(P/P_0 = 0.9)$	10.1	29	$H_{0.67}NH_{4\,1.33}$		9.49	45
				$\overline{LiNa}\cdot 3.5H_2O$	r.t. $(P/P_0 = 0.9)$	10.0	46
$\overline{HNa}\cdot 5H_2O$	r.t. $(P/P_0 = 0.7)$	11.8	39, 43	$\overline{LiNa}$	300°	7.5	38
$\overline{HNa}\cdot 4H_2O$	r.t. $(P/P_0 = 0.4)$	9.88	44				
$\overline{HNa}\cdot H_2O$	r.t. over P_4O_{10}	7.65	39	$\overline{LiK}\cdot 3H_2O$	r.t. $(P/P_0 = 0.9)$	10.0	35
$\overline{HNa}$	110°	7.33	39	$\overline{LiK}\cdot 3H_2O$	r.t. $(P/P_0 = 0.9)$	9.3	35
				$\overline{LiK}\cdot 2H_2O$	r.t. $(P/P_0 = 0.6)$	9.2	35
$\overline{HK}\cdot H_2O$	r.t. $(P/P_0 = 0.9)$	7.95	40, 43	$\overline{LiK}\cdot H_2O$	r.t. over P_4O_{10}	8.49	35
$\overline{HK}$	110°	7.50	40, 36	$\overline{LiK}$	300°	7.6	38
				$\overline{Li_{0.5}K_{1.5}}\cdot 3H_2O$	r.t. $(P/P_0 = 0.9)$	10.4	35
$H_{1.5}Rb_{0.5}\cdot 0.5H_2O$	r.t. $(P/P_0 = 0.9)$	7.60	31				
$\overline{HRb}\cdot H_2O$	r.t. $(P/P_0 = 0.9)$	8.20	31	$\overline{NaK}\cdot 3H_2O$	r.t. $(P/P_0 = 0.7)$	10.25	47
$\overline{HRb}\cdot 0.5H_2O$	r.t. over P_4O_{10}	8.20	31	$\overline{NaK}$	150°	8.04	47
$\overline{HRb}$	150°	7.60	31	$\overline{NaK}$	450°	7.9	49
$H_{0.5}Rb_{1.5}\cdot 2H_2O$	r.t. $(P/P_0 = 0.9)$	10.6	31				
$H_{0.5}Rb_{1.5}\cdot H_2O$	r.t. over P_4O_{10}	9.20	31				
$H_{0.5}Rb_{1.5}$	150°	9.16	31				

[*] r.t. = room temperature.
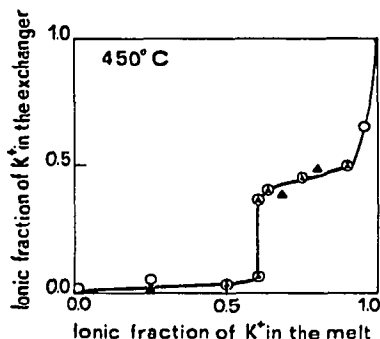
Fig. 3. Forward and reverse Na^+–K^+ ion-exchange isotherms on crystalline zirconium phosphate in molten $NaNO_3$–KNO_3 mixtures at 450° (From ref. 49). ◯, Na^+ displaces K^+ from $\overline{KK}$ (8.7 Å); ▲, K^+ displaces Na^+ from $\overline{NaNa}$ (7.7 Å).

er ion solvation are avoided and the interpretation of the ion-exchange mechanism is therefore usually simpler than in aqueous solution.

As an example, let us consider a two-step ion-exchange process, such as Na^+–K^+ exchange[49], in which a smaller counter ion is replaced with a larger one. The relative ion-exchange isotherms are shown in Fig. 3 and the entire process can be summarized as follows:
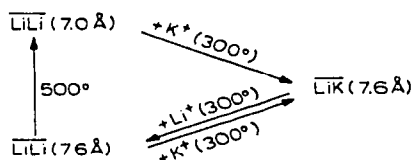
$$\overline{NaNa} \ (7.7 \ \text{Å}) \xrightarrow{K^+} \overline{NaK} \ (7.9 \ \text{Å}) \xrightarrow{K^+} \overline{KK} \ (8.9 \ \text{Å})$$
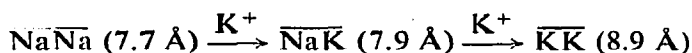
When the first Na^+ is replaced with K^+, the interlayer distance increases, in agreement with the above considerations, and an immiscible $\overline{NaK}$ phase is formed. As two solid phases are present, the degree of freedom of the system (at constant temperature and pressure) becomes zero, and therefore the exchange must occur at a constant composition of the melt; a vertical portion of the isotherm is accordingly found (see Fig. 3). The replacement of the second Na^+ with K^+ must give a new immiscible phase having a larger interlayer distance and therefore a second vertical portion of the isotherm is obtained.

The Na^+–K^+ ion exchange process at 450° seems to be reversible. However, in some ion-exchange processes, such as Li^+–K^+ (ref. 38) or Li^+–Na^+ (ref. 46) at 300°, very large hysteresis loops have been found. As already reported in a recent paper[38], the explanation could be as follows. When a larger counter ion is replacing a smaller one, the layers of the exchanger must be spread apart for space requirements. However, in the reverse process, where the smaller counter ion is replacing a larger one, the interlayer distance does not necessarily decrease again to the initial value, the formation of a metastable phase, with an interlayer distance larger than that in the original stable phase, being possible. In such a case, the exchange can occur without phase transition within a large range of the ionic composition of the solution.

A single solid phase being present, the system possesses one degree of freedom; the reverse isotherm is thus sloping and a large hysteresis loop is therefore found.

By heating the metastable solid solution at high temperature, the stable phase,

having a lower interlayer distance, is usually obtained. An example of the above considerations is the Li^+-K^+ exchange process at 300° (ref. 38):

$$\overline{LiLi}\,(7.0\,\text{Å}) \xleftarrow[\text{500°}]{} \overline{LiLi}\,(7.6\,\text{Å})$$
$$\overline{LiLi}\,(7.0\,\text{Å}) \xrightarrow{+K^+\,(300°)} \overline{LiK}\,(7.6\,\text{Å}) \xrightleftharpoons[+K^+\,(300°)]{+Li^+\,(300°)} \overline{LiLi}\,(7.6\,\text{Å})$$

where the metastable $\overline{LiLi}$ (7.6 Å) phase is obtained.

As the phase transition $\overline{LiK}$ (7.6 Å)–$\overline{LiLi}$ (7.6 Å) is reversible, the knowledge of the enthalpies involved in the single steps of the cycle could give useful information on the energy difference of a given ion-exchange process, occurring with or without change in the interlayer distance of the exchanger[50].

Ion exchange in aqueous solutions. The ion-exchange behaviour of crystalline zirconium phosphate in aqueous solutions has been extensively investigated[1,23]. Several considerations previously reported for ion-exchange processes in anhydrous media can be reconsidered here. However, in this case, one must take into account that in aqueous solution the counter ions are solvated, and consequently the interlayer distance also depends on the number of water molecules inside the exchanger. The number of the water molecules, in turn, depends on the hydration energy of the counter ion involved and on the lattice forces of the exchanger. Thus, some cases are also possible, *e.g.*, $\overline{LiLi}\cdot4H_2O$ (10.0 Å) $\xrightarrow[-H_2O]{+K^+}$ $\overline{LiK}\cdot3H_2O$ (9.3 Å)[35], in which the interlayer distance decreases when a smaller counter ion is replaced with another ion having a larger radius but a lower hydration energy.

From a general point of view, when an ion-exchange process occurs with a phase transition, giving rise to an ionic form having a larger interlayer distance than the original one, the formation of a metastable supersaturated solid solution is possible in the reverse process and, as a consequence, a hysteresis loop can be obtained. Small hysteresis loops have been found for the Na^+-K^+ exchange system[34,47], while very large hysteresis loops are found for systems such as Li^+-K^+ (ref. 35), Rb^+-H^+ and Cs^+-H^+ (ref. 31). In the former case, the small hysteresis loop is explained by assuming, as in the case of zeolites[51], that the phase rearrangement is delayed by a potential activation energy; therefore, phase transition takes place only when the original solid phase has been supersaturated by the incoming counter ion. Thus the forward and reverse isotherms do not coincide, as the phase rearrangement in the two opposite processes occurs at different ionic compositions of solution. In the latter cases, the large hysteresis loops were due to the formation of different phases in the two opposite processes, as already discussed for ion exchange in molten salts.

A comparison of titration curves of $\overline{HH}\cdot H_2O$ (7.6 Å) with alkali metal hydroxides is shown in Fig. 4. The X-ray analyses of samples at various stages of exchange have demonstrated that: (*a*) Na^+ and K^+ are exchanged in two steps in the approximate ranges 0–50% and 50–100% of conversion; (*b*) Li^+ is exchanged in three steps (0–50%, 50–75% and 75–100%); (*c*) Rb^+ is exchanged in three steps (0–25%, 25–75% and 75–100%); and (*d*) Cs^+ is exchanged in four steps (0–25%, 25–50%, 50–75% and 75–100%).

Percent of conversion
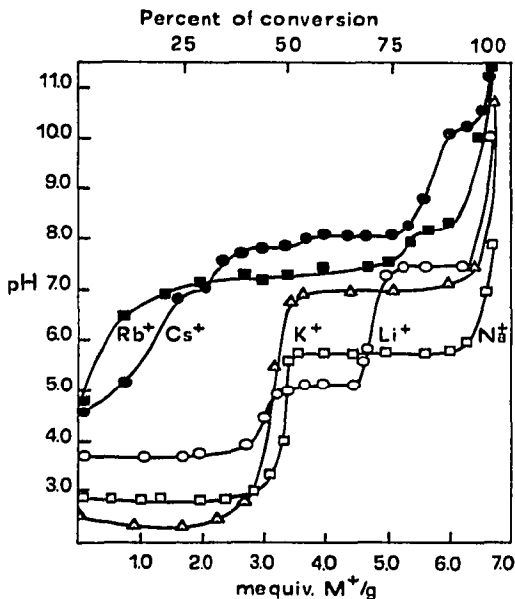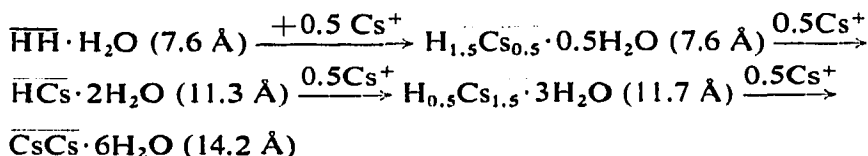

Fig. 4. Comparison of titration curves of crystalline zirconium phosphate with alkali metal ions. Conditions: 1 g of $\overline{HH} \cdot H_2O$ (7.6 Å) in 200 ml of 0.1 N (MCl + MOH) solution at 25 ± 1°.

The reasons for which crystalline zirconium phosphate exhibits different functionalities for the various alkali metal ions can most likely be ascribed to steric hindrance. As an example, we will try to explain the Cs^+–H^+ exchange on the basis of the crystal structure of zirconium phosphate. As already reported in a previous paper[31], this process can be summarized as:

$$\overline{HH} \cdot H_2O \ (7.6 \ Å) \xrightarrow{+0.5 \ Cs^+} H_{1.5}Cs_{0.5} \cdot 0.5H_2O \ (7.6 \ Å) \xrightarrow{0.5Cs^+}$$

$$\overline{HCs} \cdot 2H_2O \ (11.3 \ Å) \xrightarrow{0.5Cs^+} H_{0.5}Cs_{1.5} \cdot 3H_2O \ (11.7 \ Å) \xrightarrow{0.5Cs^+}$$

$$\overline{CsCs} \cdot 6H_2O \ (14.2 \ Å)$$

It can be pointed out that in the first ion-exchange step, a solid solution is formed and the interlayer distance remains constant. By taking into account the spatial arrangement of the fixed O^- charges, it can easily be seen that this is possible only if a Cs ion enters inside the cavity where, for the interlayer distance of 7.6 Å, there is sufficient space to accommodate a Cs ion. Thus the water originally present near the centre of the cavity must be displaced, and therefore for each Cs^+ taken up by the exchanger, one molecule of water must be lost, as indeed is found[31]. Furthermore, owing to electrostatic repulsion, the unexchanged proton originally present in the cavity must be displaced away from the Cs ion, and it probably moves towards an adjacent cavity. At a degree of Cs^+ exchange of 25%, a situation similar to that shown schematically in Fig. 5 may be reached: 50% of the cavities are filled with a single Cs ion while the remaining cavities contain one water molecule and an average of three hydrogen ions.

In the second step, a degree of conversion of 50% is reached and each of the
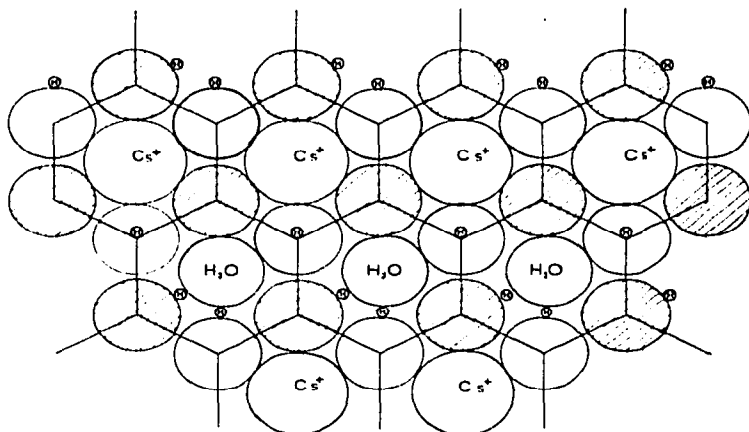
Fig. 5. Proposed arrangement of fixed charges, counter ions and water molecules in the phase $\overline{H_{1.5}Cs_{0.5}}\cdot0.5H_2O$ (7.6 Å), viewed in a planar projection as described in Fig. 2.

cavities will therefore contain one Cs^+ placed near the centre, while the unexchanged protons, for electrostatic repulsion, are likely to be displayed towards the side of the cavities. The interlayer distance increases to 11.3 Å and water can enter inside the exchanger[31].

As the pH is further increased other H^+ ions of the $\overline{HCs\cdot2H_2O}$ (11.3 Å) phase are exchanged and therefore more than one Cs^+ for each cavity has to be accommodated. In this case, Cs ions can no longer remain near the centre of the cavities and, for space requirements, the interlayer distance increases considerably. The presence of 25 % of a small counter ion, such as H^+, allows the Cs ions to remain further inside the cavities; consequently, the 75 % loading Cs^+ phase can have an interlayer distance appreciably lower than that of the completely exchanged Cs^+ form in which, for space requirements, Cs ions are obliged to move towards the external part of the cavities[41]. The 75 % Cs^+-loaded phase must, however, be highly disordered, as confirmed by X-ray diffraction patterns[31].

Finally, at very high pH values, the energy is sufficient to form the completely exchanged $\overline{CsCs\cdot6H_2O}$ phase (fourth step). Using eqn. 2, it is possible to calculate that the interlayer distance of this phase must be 13.8 Å, which is in good agreement with the experimental value of 14.2 Å. This phase must again become ordered, as indeed is confirmed by its X-ray powder pattern.

Steric hindrance and ion selectivity for large cations on crystalline zirconium phosphate

As reported above, the maximum diameter of the windows interconnecting adjacent cavities of $\overline{HH\cdot H_2O}$ (7.6 Å) is 2.64 Å. Hence the ions that have a crystalline diameter greater than this value should not be exchanged for steric hindrance reasons. However, if sufficient energy is supplied, e.g., by increasing the pH of the solution, the layers can spread apart and the large ions enter inside the exchanger. We have already seen that Rb^+ and Cs^+ can be taken up by $\overline{HH\cdot H_2O}$ (7.6 Å) until complete conversion occurs, although the exchange needs high pH values.

For this reason, crystalline zirconium phosphate has been regarded as a poor ion exchanger for large cations and, until recently, ion-exchange experiments have been
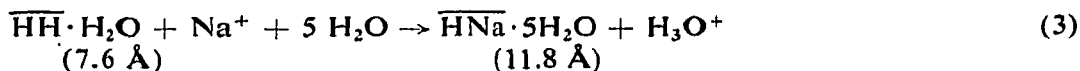
limited to only a few cations, such as Li^+, Na^+, K^+, NH_4^+, Ca^{2+} and Sr^{2+}. However, it was recently found in our laboratory[43,52] that large cations can be easily exchanged with crystalline zirconium phosphate if steric hindrances are removed, e.g., by using some ionic form that has a very large interlayer distance.

By employing $\overline{HNa} \cdot 5H_2O$ (11.8 Å), it was not only observed that the Na^+ was was easily replaced with Rb^+, Cs^+ or Ba^{2+} (refs. 43 and 53), but also that large ions were strongly preferred by the exchanger. Taking into account that Na^+ is easily exchanged with $\overline{HH} \cdot H_2O$, it can be concluded that the ion exchange of large cations by this exchanger requires a high activation energy due to steric hindrance. Once these steric hindrances are removed, the ion-exchange activation energy decreases and large cations can be exchanged. Now, it is well known that although the rate of a chemical reaction that needs a high activation energy is very low, its rate can be increased appreciably if a suitable catalyst is added. Therefore, it was worthwhile to investigate if an ion-exchange process that needs a high activation energy can be accelerated by adding a suitable ion-exchange catalyst.
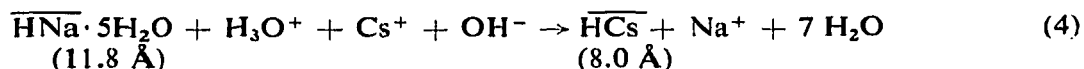
Taking into account the earlier results with $\overline{HNa} \cdot 5H_2O$, we investigated the exchange of large cations with $\overline{HH} \cdot H_2O$ (7.6 Å) in the presence of small amounts of Na^+ (ref. 54). It was found that Na^+ behaves as an ion-exchange catalyst in so far as the exchange of large cations occurs, or is accelerated, in the presence of small amounts of Na^+; furthermore, it is not consumed in the overall ion-exchange reaction as all the Na^+ added is found in solution at the end of the process.

We suggest the following mechanism, already reported[54] and confirmed by successive experiments[55], for the catalytic effect of Na^+ on the exchange of a large cation, M^+.

Primarily, Na^+ is exchanged with $\overline{HH} \cdot H_2O$ (7.6 Å):

$$\overline{HH} \cdot H_2O + Na^+ + 5\ H_2O \rightarrow \overline{HNa} \cdot 5H_2O + H_3O^+ \qquad (3)$$
$$\text{(7.6 Å)} \qquad\qquad\qquad \text{(11.8 Å)}$$

When an appreciable amount of $\overline{HNa} \cdot 5H_2O$ (11.8 Å) phase is formed, the large cation M^+ can be exchanged with $\overline{HNa} \cdot 5H_2O$; e.g. if M^+ is Cs^+, we have:

$$\overline{HNa} \cdot 5H_2O + H_3O^+ + Cs^+ + OH^- \rightarrow \overline{HCs} + Na^+ + 7\ H_2O \qquad (4)$$
$$\text{(11.8 Å)} \qquad\qquad\qquad\qquad \text{(8.0 Å)}$$

The Na^+ replaced with Cs^+ can give a new $\overline{HNa} \cdot 5H_2O$ phase according to process 3 and so on, until all of the $\overline{HH} \cdot H_2O$ phase is converted into the $\overline{HCs}$ phase. The uptake of large cations by enlarged zirconium phosphate phases, as well as Na^+-catalysed processes, indicates new practical applications for such exchangers, which can now be employed in ion-exchange procedures involving important cations such as Cs^+, UO_2^{2+} and various transition metal ions.

Ion-exchange mechanism for crystalline zirconium phosphate for polyvalent ions

So far, very little experimental work on the ion exchange of polyvalent ions has been carried out[36,56–58]. It was found that Mg^{2+} and Ba^{2+} are not appreciably exchanged by $\overline{HH} \cdot H_2O$ (7.6 Å) at room temperature[57]; instead, Sr^{2+} and Ca^{2+} are

slowly exchanged at acidic pH values to form phases with the approximate composi-
tion $H_{0.9}Sr_{0.55} \cdot 3.5H_2O$ (10.2 Å) and $H_{0.74}Ca_{0.63} \cdot 3H_2O$ (10.0 Å), respectively. The
complete conversion to Ca^{2+} or Sr^{2+} forms seems to require high pH values; however
hydrolysis of the exchanger and precipitation of calcium or strontium phosphate
occurs at pH values higher than about 5, so preventing the completely exchanged
phases from being obtained.

Considerable progress in the ion exchange of divalent ions has recently been
accomplished by using some zirconium phosphate phases having a large interlayer
distance, such as the mixed salt form $\overline{HNa} \cdot 5H_2O$ (11.8 Å)[53,54].

It has indeed been possible, using this exchanger, to obtain a completely
converted $\overline{Ba} \cdot 3.0H_2O$ (9.4 Å) phase[53] and some partially converted phases containing
Mg^{2+} (ref. 54), UO_2^{2+} (ref. 52) and transition metal ions of the first series[59]. Further-
more, these studies have shown that divalent ions are strongly preferred to Na^+ and
therefore, as already discussed for large monovalent ions, the lack of exchange by
$\overline{HH} \cdot H_2O$ (7.6 Å) for Ba^{2+}, Mg^{2+} or transition metal ions should be essentially due
to steric hindrance (e.g., the large crystalline radius of Ba^{2+} or too large a hydrated
ionic radius and high energy of hydration for other divalent ions).
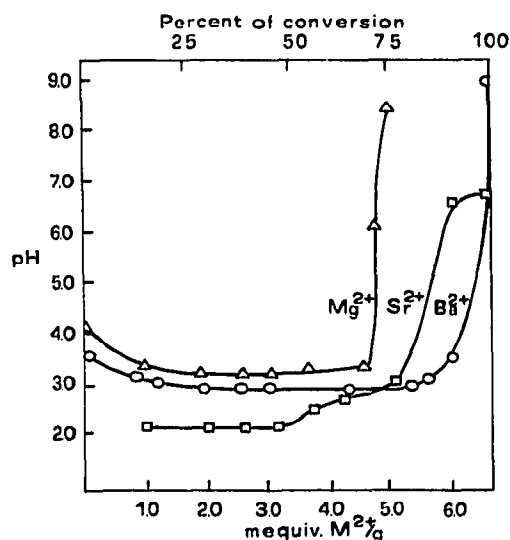
Fig. 6. Comparison of titration curves of crystalline zirconium phosphate with alkaline earth metal
ions. Conditions: 1 g of $\overline{HH} \cdot H_2O$ (7.6 Å) in 200 ml of 0.1 N (MCl_2 + $M(OH)_2$) solution at 25 ±
1°, in the presence of $5 \cdot 10^{-3}$ M NaCl as catalyst.

Hence the exchange of these ions by $\overline{HH} \cdot H_2O$ could be made possible in the
presence of small amounts of Na^+, and this was indeed found true for Mg^{2+} and Ba^{2+}
(refs. 53 and 54). It is interesting to compare the titration curves of alkaline earth
metal ions on $\overline{HH} \cdot H_2O$ (7.6 Å) in the presence of added Na^+ (see Fig. 6).

X-ray analyses showed that the following phase transitions take place at acidic
pH values:

$$\overline{HH} \cdot H_2O \xrightarrow{+0.55 \ Sr^{2+}} H_{0.9}Sr_{0.55} \cdot 3.5H_2O$$
$$(7.6 \ \text{Å}) \qquad\qquad\qquad (10.2 \ \text{Å})$$

$$\overline{HH} \cdot H_2O \xrightarrow{0.63 \ Ca^{2+}} H_{0.74}Ca_{0.63} \cdot 3H_2O$$
$$(7.6 \ \text{Å}) \qquad\qquad\qquad (10.0 \ \text{Å})$$

$$\overline{HH} \cdot H_2O \xrightarrow{0.72 \ Mg^{2+}} H_{0.56}Mg_{0.72} \cdot 4H_2O$$
$$(7.6 \ \text{Å}) \qquad\qquad\qquad (9.85 \ \text{Å})$$

$$\overline{HH} \cdot H_2O \xrightarrow{Ba^{2+}} \overline{Ba} \cdot 3.0H_2O$$
$$(7.6 \ \text{Å}) \qquad\qquad (9.4 \ \text{Å})$$
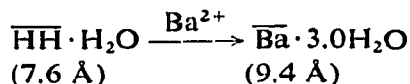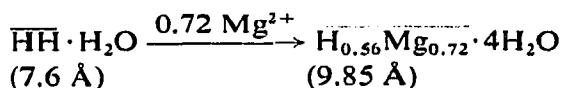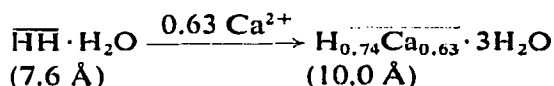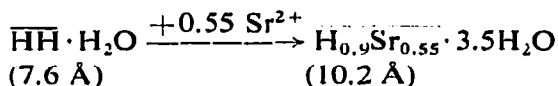
Owing to the lack of structural data for divalent salt forms, it is not possible at present to discuss in detail the ion-exchange mechanism of these ions on crystalline zirconium phosphate. However, in case these data do not become available, the interlayer distances must be carefully considered in order to make some general assumptions on the reticular position of divalent ions and to draw some conclusions on their ion-exchange mechanism.

A preliminary inspection of the data in Table IV shows that the interlayer distance of the anhydrous $\overline{Ba}$ form is very low and therefore it is likely that Ba^{2+} is accommodated near the centre of the cavity. In such a case, Ba^{2+} will be coordinated by the six oxygen atoms carrying negative charges. This fact could also explain the high selectivity of zirconium phosphate for this ion. Furthermore, as each Ba^{2+} is accommodated in one cavity, the ion-exchange process should occur in a single step, as is found experimentally[53].

In the case of smaller divalent ions, owing to their high hydration energy, it seems that their position is shifted out from the centre of the cavity, as phases at degrees of conversion of 50%, 66% and 75%, which correspond to filling of 1/2, 2/3 and 3/4 of the total cavities, are also possible. Finally, as regards the ion exchange of trivalent ions, preliminary investigations in progress in our laboratory[52] have shown that Tl^{3+} and Cr^{3+} are negligibly exchanged by $\overline{HH} \cdot H_2O$ (7.6 Å). As trivalent ions are taken up instead by amorphous zirconium phosphate[3], it is likely that the exchange of these ions on crystalline zirconium phosphate requires a high activation energy. For this reason, we are now investigating the ion exchange of trivalent cations by using enlarged forms of crystalline zirconium phosphate, and preliminary experiments on the exchange of Tl^{3+} and La^{3+} on $\overline{HNa} \cdot 5H_2O$ (11.8 Å) seem to confirm that partially converted forms with trivalent cations can be obtained[52].

Diffusion of counter ions and electrical conductivity of crystalline zirconium phosphate
Very little experimental work has been carried out in such important fields[58,61]. We have already seen that the uptake of large ions by an exchanger having a low interlayer distance requires a high activation energy. Their ion-exchange kinetics are therefore expected to be very slow, as indeed is found experimentally[54] for Cs^+ exchange on $\overline{HH} \cdot H_2O$ (7.6 Å). The rate of exchange should increase by increasing the interlayer distance of the exchanger, and this expectation has been confirmed by study-

TABLE IV

INTERLAYER DISTANCES OF HYDRATED AND ANHYDROUS DIVALENT IONIC FORMS OF CRYSTALLINE ZIRCONIUM PHOSPHATE

Alkaline earth metal ions

Phase composition	Drying conditions*	Interlayer distance, $d(Å)$	Ref.
$Mg_{0.72}H_{0.56} \cdot 4H_2O$	r.t. $(P/P_0 = 0.9)$	9.85	54
$Mg_{0.72}H_{0.56}$	180°	7.69	53
$Ca_{0.65}H_{0.74} \cdot 3H_2O$	r.t. $(P/P_0 = 0.7)$	9.98	57
$\overline{Ca_{0.63}H_{0.74}}$	200°	7.46	57
$Sr_{0.5}H \cdot 4H_2O$	r.t. $(P/P_0 = 0.9)$	10.2	53
$\overline{Sr_{0.5}H}$	200°	7.46	53
$\overline{Ba \cdot 3.0H_2O}$	r.t. $(P/P_0 = 0.9)$	9.4	53
$\overline{Ba}$	200°	7.55	53

Transition metal ions

Phase composition	Drying conditions	Interlayer distance, $d(Å)$	Ref.
$\overline{Mn_{0.63}H_{0.74} \cdot nH_2O}$	Wet sample	9.75	59
$\overline{Mn(II)}$	160°	7.41	60
$\overline{Co_{0.57}H_{0.86} \cdot nH_2O}$	Wet sample	10.30	59
		9.93	59
$\overline{Co(II)}$	160°	7.41	60
$\overline{Ni_{0.76}H_{0.48} \cdot nH_2O}$	Wet sample	9.82	59
$\overline{Cu_{0.78}H_{0.44} \cdot nH_2O}$	Wet sample	9.50	59
$\overline{Cu_{0.78}H_{0.44}}$	320°	7.91	59
$\overline{Cu(II)}$	260°	7.87	60
$\overline{Zn_{0.74}H_{0.52} \cdot nH_2O}$	Wet sample	9.65	59
$\overline{Zn}$	115°	7.41	60

* r.t. = room temperature.

ing the uptake of Cs^+ on $\overline{HNa} \cdot 5H_2O$ (11.8 Å) phase or on $\overline{HH} \cdot H_2O$ (7.6 Å) in the presence of Na^+ as a catalyst.

In our laboratory, determinations of the electrical conductivity of zirconium phosphate of different degrees of crystallinity and in several ionic forms are also in progress. Preliminary results[62] seem to indicate that the conductivity of $\overline{HH} \cdot H_2O$ (7.6 Å) increases with increasing degree of disorder in the crystal structure (see Table V).

TABLE V

SPECIFIC ELECTRICAL CONDUCTIVITY OF SOME IONIC FORMS OF ZIRCONIUM PHOSPHATE

Exchanger	Preparation	Specific conductivity $(ohm^{-1}\ cm^{-1})$
$Zr(HPO_4)_2 \cdot nH_2O$	Amorphous	$8.4 \cdot 10^{-3}$
$Zr(HPO_4)_2 \cdot H_2O$	Refluxed for 100 h in 10 M H_3PO_4	$9.4 \cdot 10^{-5}$
$Zr(HPO_4)_2 \cdot H_2O$	HF method	$4.2 \cdot 10^{-5}$
$Zr(NaPO_4)_2 \cdot 3H_2O$	HF method	$2.2 \cdot 10^{-4}$
$ZrMg_{0.72}H_{0.50}(PO_4)_2 \cdot 4H_2O$	HF method	$1.3 \cdot 10^{-5}$

However, a comparison among the conductivity values is difficult because, owing to the low conductivity of truly crystalline materials, the surface conductivity becomes appreciable. On the other hand, the surface area also increases with decreasing crystallinity and this effect on the overall conductivity must be taken into account. Nevertheless, by determining the relative values of the surface areas of the various samples, it was possible to establish that the decrease in conductivity with increasing degree of crystallinity was greater than the decrease in surface area.

It can also be noted that the conductivity of the Ba^{2+} form of crystalline zirconium phosphate is very low. In agreement with this result, we have found that the rate of the ion-exchange processes

$$\overline{Ba} + M^{2+} \rightarrow Ba^{2+} + \overline{M}$$
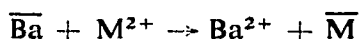
where M = Mg, Ca or Sr is very low[53].

Other exchangers having a layered structure

In recent years, systematic investigations on the synthesis of insoluble crystalline acid salts of tetravalent metals led to the preparation of several new crystalline ion exchangers other than zirconium phosphate. The exchangers that have a layered structure are listed in Table I.

Their ion-exchange properties have been studied less frequently than those of zirconium phosphate; however, owing to the similarity between their crystalline structure and that of zirconium phosphate, we will try to discuss some expected ion-exchange behaviour.

In our opinion the ion exchange properties to be expected are:

(*a*) Dependence of the interlayer distances of exchanged ionic forms on the counter ion radius and water content.

(*b*) Occurrence of phase transitions and, consequently, ion exchange at fixed composition of the solution (plateau in the titration curves and vertical portions on the ion-exchange isotherms).

(*c*) Formation of metastable phases and, consequently, ion-exchange irreversibility and hysteresis loops between forward and reverse processes.

(*d*) High activation energy in the ion exchange of large cations and catalytic effect of small amounts of Na^+ or Li^+.

Some properties already reported in previous papers[8-12] and some preliminary data on crystalline titanium phosphate[63] are in good agreement with the above expectations.

In our opinion, another interesting aspect of layered exchangers is the study of the relative variations in their ion-exchange behaviour as a function of the tetravalent metal and the polybasic acid involved.

Let us examine first the influence of the substitution of zirconium with other tetravalent metals. We have already seen that three oxygen atoms of each phosphate group are bonded to three tetravalent metal atoms lying in a plane. When zirconium is replaced with a smaller tetravalent metal such as titanium, smaller cavities (and consequently smaller windows connecting the cavities) have to be expected, as the Ti–O distance is shorter than the Zr–O distance and therefore the Ti–Ti distance in the plane of metal atoms should be shorter than Zr–Zr distance. It was recently reported by Clearfield *et al.*[23] that the Ti–Ti and Zr–Zr distances in the corresponding phosphates are 5.3 and 5.0 Å, respectively. Hence the ion exchange of large cations by crystalline titanium phosphate should require an even higher activation energy than in zirconium phosphate. As previously reported[15], ion-sieve effects are higher in titanium than in zirconium phosphate.

The substitution of zirconium atoms with a larger tetravalent metal is expected to give an exchanger with slightly larger cavities. However, by substituting Zr with Ce(IV) or Th(IV), a fibrous structure has been obtained instead of the layered structure.

Let us now examine the effect of the substitution of the phosphate group with a larger polybasic acid group such as arsenate. We believe that the following changes in the ion-exchange properties could be expected:

(*a*) The Zr–Zr distance in zirconium arsenate should be longer than in zirconium phosphate; therefore, the cavities should also be larger, with a smaller steric hindrance than in zirconium phosphate. The Zr–Zr distances in zirconium arsenate and phosphate are 5.378 and 5.307 Å, respectively[23]. The exchange of Ba^{2+} ion by zirconium arsenate[8], but not by zirconium phosphate[57], could be related to the larger cavities in the former exchanger.

(*b*) The interlayer distance of M(IV) arsenates should be greater than in the corresponding M(IV) phosphates, as the As–O distance is greater than the P–O distance. As already shown in Table I, the interlayer distances of zirconium arsenate and phosphate are 7.82 and 7.56 Å, while those of titanium arsenate and phosphate are 7.77 and 7.56 Å, respectively.

(*c*) The hydrolysis should increase as the size of the polybasic acid group increases. In agreement with this view, it was found that crystalline titanium arsenate is a more hydrolyzable exchanger than crystalline titanium phosphate[12].

(*d*) Some differences in ion-exchange selectivity could also be expected be-

cause, according to the Eisenman theory[64], ion selectivity also depends on the field strength of the anions involved carrying the fixed charges.

Finally, the dimensions of the polybasic acid involved could play an important role in determining the crystalline structure of the exchanger. As an example, it can be pointed out that a phosphate group, with its small size, could be unable to bind three large tetravalent metals lying in a plane. Such a situation could instead be possible for other polybasic groups larger than phosphate, such as arsenate or antimonate. In this respect, it is interesting to note that cerium(IV) and thorium phosphates have a fibrous structure while the corresponding arsenates give microcrystals with as yet unknown structures (see Table VI). To understand the reasons for which a combination of a given tetravalent metal and a given polybasic acid gives a characteristic crystalline structure is of the utmost importance and studies in this field will also be very useful in the synthesis of new inorganic exchangers.

TABLE VI

ION EXCHANGERS HAVING AS YET UNKNOWN STRUCTURES

Formula	Theoretical ion-exchange capacity (mequiv. H^+/g)	First X-ray diffraction maxima, d ($\AA$)	References
$Sn(HPO_4)_2 \cdot H_2O$	6.08	7.76	17, 18
$Sn(HAsO_4)_2 \cdot H_2O$	4.80	7.77	17
$Ce(HPO_4)_2 \cdot 1.33H_2O$	5.78	15.9	19
$Ce(HAsO_4)_2 \cdot 2H_2O$	4.38	10.1	14
$Th(HAsO_4)_2 \cdot H_2O$	3.78	7.05	15

FIBROUS INORGANIC ION EXCHANGERS

Cerium(IV) phosphate[10] and thorium phosphate[65] are the only two insoluble acid salts of tetravalent metals having a fibrous structure that have so far been synthesized. Fig. 7 shows an electron micrograph of a sample of cerium(IV) phosphate, showing its fibrous nature.

Fibrous inorganic ion exchangers are very interesting because they can be used to prepare inorganic ion-exchange papers or thin layers suitable for chromatographic separations as well as inorganic ion-exchange membranes without a binder. These applications will be discussed later, while below some properties of these exchangers, mainly referred to cerium(IV) phosphate, are reported.

Synthesis and composition of fibrous exchangers

These exchangers have been synthesized by adding slowly a solution of a Ce(IV) or Th(IV) salt to a hot solution (80–100°) of orthophosphoric acid with constant stirring. The effect of the temperature and digestion time, as well as of the molar ratio $PO_4/Ce(IV)$ or PO_4/Th in solution, has already been reported in previous papers[10,65].
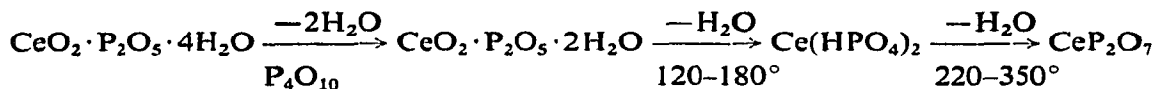
Unfortunately, so far it has not been possible to establish the structure of cerium(IV) or thorium phosphate because single fibres of suitable size for X-ray studies

Fig. 7. Electron micrograph of a sample of fibrous cerium(IV) phosphate (magnification 10,000 ×).

have not yet been obtained; even the chemical formula is not known for certain. However, some information has been derived from chemical and thermal analyses, ion-exchange properties, X-ray diffraction patterns and recently infrared spectroscopy[66,67].

The chemical composition of cerium(IV) phosphate is $CeO_2 \cdot P_2O_5 \cdot 4H_2O$ and its thermal behaviour can be summarized as:

$$CeO_2 \cdot P_2O_5 \cdot 4H_2O \xrightarrow[P_4O_{10}]{-2H_2O} CeO_2 \cdot P_2O_5 \cdot 2H_2O \xrightarrow[120-180°]{-H_2O} Ce(HPO_4)_2 \xrightarrow[220-350°]{-H_2O} CeP_2O_7$$

The first step of the dehydration process does not cause significant changes in the X-ray powder pattern, but at 180° the material becomes almost amorphous and friable.

The molecule of water lost at about 180° is essential to the fibrous structure and, as infrared spectroscopy gives evidence for the formula $Ce(HPO_4)_2 \cdot 3 H_2O$, this water molecule could join the fibres through hydrogen bonds.

Ion-exchange properties

Recently, extensive studies have been undertaken in this laboratory to determine the ion-exchange properties of fibrous cerium(IV) phosphate towards several monovalent, divalent and trivalent cations[67]. In the preliminary results of these studies (Fig. 8), the ion uptake curves do not show any definite plateau, and the mechanism of exchange seems to occur without phase transitions and the exchangeable hydrogen ions display a large range of acidities like amorphous or semicrystalline exchangers. Fibrous cerium(IV) phosphate shows, at low loading, the sequence of the lyotropic series $Cs^+ > K^+ > Na^+ > Li^+$ or $Ba^{2+} > Sr^{2+} > Ca^{2+} > Mg^{2+}$, while, on increasing the loading of the exchanger, several reversals in selectivity occur until the sequence is almost completely reversed. It can be pointed out that with cations that
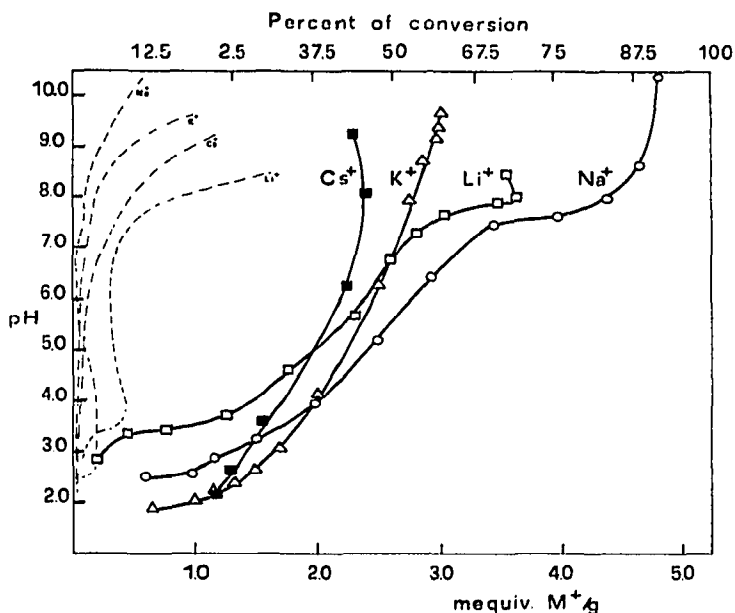
Fig. 8. Uptake and hydrolysis curves of fibrous cerium(IV) phosphate with alkali metal ions. Abscissae: uptake (solid lines), mequiv. M^+ per gram of exchanger; hydrolysis (dashed lines), mmoles of phosphate groups released by 1 g of exchanger to the solution. Conditions: 1 g of fibrous cerium(IV) phosphate in 200 ml of 0.1 N (MCl + MOH) solution at 25 ± 1°.

have a large crystalline radius, such as K^+ and Cs^+, conversions higher than 50%
cannot be obtained in an acidic medium and, when the pH is increased to alkaline
values, the exchanger hydrolyzes appreciably. As it is difficult to imagine that ion sieve
exclusion would occur in a fibrous structure, this phenomenon could be ascribed, for
example, to steric factors due to the closeness of adjacent fixed charges. It is notable
that no sieving effect has been found for large divalent ions such as Ba^{2+}; the X-ray
powder pattern has only a few lines, of which the first is much more intense than the
others. Its value ($d = 11.2$ Å) changes very little as the exchanging ion or the degree
of exchange is changed, thus supporting the hypothesis that ion-exchange processes
occur without phase transitions, as if a solid solution were formed.

Support-free fibrous cerium(IV) phosphate sheets have been used for the
chromatographic separation of inorganic ions[68]. In order to obtain more quantitative
information on the selectivity of the fibrous cerium phosphate, K_d values of various
inorganic ions at different concentrations have been determined[67]. In Table VII, some
of these results are reported. The marked selectivity towards ions such as Pb^{2+}, Ag^+
and Co^{2+} can be pointed out, so that this exchanger could be employed for several
separations of analytical interest. Furthermore, as the increase in K_d values with
decreasing concentration is different for the various ions, better separations could be
obtained in diluted solution.

Owing to the presence of Ce(IV) in the exchanger, redox reactions may take
place with highly reducing ions. This behaviour, already found for Mn^{2+} in amorphous
cerium phosphate[69], has also been confirmed for other ions such as Fe^{2+} and Cr^{3+}.

TABLE VII

DISTRIBUTION COEFFICIENT (mequiv. M^+/g: mequiv. M^+/ml) OF VARIOUS INORGANIC IONS ON FIBROUS CERIUM(IV) PHOSPHATE AT 25 ± 1° (g/ml = 25)

Ion	Concentration (N)		
	10^{-2}	$5 \cdot 10^{-3}$	10^{-3}
Na^+	32.2	50.3	122
Ag^+	215	325	550
Pb^{2+}	$7.8 \cdot 10^3$	10^6	10^6
Cu^{2+}	125	230	$1.3 \cdot 10^3$
Co^{2+}	33	43	100
Cr^{3+}	100	350	10^4

SOME PRACTICAL APPLICATIONS OF CRYSTALLINE INORGANIC ION EXCHANGERS OF THE CLASS OF INSOLUBLE ACID SALTS OF TETRAVALENT METALS

So far, very little experimental work on the practical applications of these crystalline exchangers has been carried out because, as already discussed, they have been considered to be, until recently, poor exchangers for large cations.

The discovery that these cations can be exchanged by enlarged phases of crystalline zirconium phosphate, indicates many new possibilities for the practical application of such exchangers.

Fig. 9 shows the Na^+–Sr^{2+} isotherm obtained by using $ZrHNa(PO_4)_2 \cdot 5H_2O$ (11.8 Å).

The ion-exchange process takes place with the following single phase transition:

$$\underset{(11.8 \text{ Å})}{HNa \cdot 5H_2O} \xrightarrow{0.5 \; Sr^{2+}} \underset{(10.2 \text{ Å})}{\overline{HSr_{0.5}} \cdot 4H_2O}$$

and the isotherm is therefore almost completely vertical. It can be seen that the phase transition occurs at a very low Sr^{2+} ionic fraction in solution and thus Sr^{2+} is strongly

Fig. 9. Na^+–Sr^{2+} forward ion-exchange isotherms on $HNa \cdot 5H_2O$ (11.8 Å). Concentration: 0.01 N. Temperature: 25 ± 1°.

preferred to Na^+. Similar results have been obtained with Ca^{2+}, while the preference for Ba^{2+} is even greater[53]. In our opinion, some practical applications of $\overline{HNa} \cdot 5H_2O$ (11.8 Å) in water softening by alkaline earth metals or other divalent metal ions could be possible.

Further, we have seen above that $\overline{HNa} \cdot 5H_2O$ can exchange several divalent transition metal ions; investigations on the catalytic activity of zirconium phosphate phases loaded with transition metal ions seem to be very promising[70]. An interesting application of the layered exchangers could be to act as solid buffers. We have seen before that the conversion of $\overline{HH} \cdot H_2O$ in a given salt form usually occurs with a phase transition and therefore the pH of the solution has to remain constant until all of the $\overline{HH} \cdot H_2O$ phase is completely converted into the new ionic form. It can be pointed out that the conversion of a given salt form into another form occurs also with phase transition and, consequently, at constant composition of the solution. Hence the layered exchangers could also be employed in order to keep constant the ionic fraction of cations involved in the exchange.

The very high selectivity of fibrous exchangers towards Pb^{2+} and certain other divalent cations is also very promising for practical applications[67]. At present, investigations are in progress in this laboratory in order to examine the practical application of fibrous cerium(IV) phosphate in the removal of some heavy metal ions from industrial waters. Inorganic ion-exchange papers are also suitable supports for carrying out good chromatographic or electrophoretic separations of inorganic ions.

Some exchangers that as yet have an unknown structure also possess interesting ion-sieve properties; *e.g.*, thorium arsenate behaves as a very narrow ion sieve: its protons being exchanged only by anhydrous Li^+ (ref. 15).

This interesting property has already been employed for carrying out good separations of Li^+ from other cations, even if present in high concentrations, and a practical application in the recovery of Li^+ from natural waters and dilute solutions can also be expected.

Finally, the insoluble acid salts of tetravalent metals have been employed for preparing inorganic ion-exchange membranes. These membranes are interesting from both a fundamental and a practical point of view. They represent a unique possibility for relating their electrochemical and osmotic properties to the known reticular arrangement of the fixed charges and counter ions or to steric factors. On the other hand, owing to the selectivity and stability of inorganic exchangers, these membranes could have applications as selective electrodes or in particular processes in which organic membranes cannot be employed because of their higher degradability. Particularly promising could be their employment in fuel cells at high temperatures or in the concentration of wastes containing fission products.

Extensive research on inorganic ion-exchange membranes is in progress in our laboratory under a C.N.R. contract, in order to investigate their electrochemical properties and particularly to examine their application in the desalting of brackish waters. Some of the membranes examined, in particular Ce(IV) phosphate membranes without a binder, seem to possess good electrochemical properties.

CONCLUSION

Recent advances with insoluble crystalline acid salts of tetravalent metals have

revealed several important fundamental aspects of these exchangers. However, further investigations, especially of a structural and thermodynamic nature, are still needed in order to understand in detail their ion-exchange mechanism and to make some predictions about their ion-exchange properties. Furthermore, as already discussed, the exchange of large cations by enlarged layered exchangers has opened new possibilities for the practical application of these exchangers and this will certainly be a stimulus for further investigations.

ACKNOWLEDGEMENTS

REFERENCES

1 V. Veselý and V. Pekárek, *Talanta*, 19 (1972) 219.
2 V. Veselý and V. Pekárek, *Talanta*, 19 (1972) 1245.
3 C. B. Amphlett, *Inorganic Ion Exchangers*, Elsevier, Amsterdam, 1964.
4 A. Clearfield and J. A. Stynes, *J. Inorg. Nucl. Chem.*, 26 (1964) 117.
5 A. Winkler and E. Thilo, *Z. Anorg. Allg. Chem.*, 346 (1966) 92.
6 G. Alberti, P. Cardini Galli, U. Costantino and E. Torracca, *J. Inorg. Nucl. Chem.*, 29 (1967) 571.
7 K. H. Konig and E. Meyn, *J. Inorg. Nucl. Chem.*, 29 (1967) 1153.
8 E. Torracca, U. Costantino and M. A. Massucci, *J. Chromatogr.*, 30 (1967) 584.
9 G. Alberti and E. Torracca, *J. Inorg. Nucl. Chem.*, 30 (1968) 317.
10 G. Alberti, U. Costantino, F. di Gregorio, P. Galli and E. Torracca, *J. Inorg. Nucl. Chem.*, 30 (1968) 295.
11 A. Clearfield, G. D. Smith and B. Hammond, *J. Inorg. Nucl. Chem.*, 30 (1968) 277.
12 G. Alberti and E. Torracca, *J. Inorg. Nucl. Chem.*, 30 (1968) 3073.
13 A. Clearfield, R .H. Blessing and J. A. Stynes, *J. Inorg. Nucl. Chem.*, 30 (1968) 2249.
14 G. Alberti, U. Costantino, F. di Gregorio and E. Torracca, *J. Inorg. Nucl. Chem.*, 31 (1969) 3195.
15 G. Alberti and M. A. Massucci, *J. Inorg. Nucl. Chem.*, 32 (1970) 1719.
16 E. Torracca, G. Alberti, R. Platania, P. Scala and P. Galli, in *Ion Exchange in the Process Industries*, Society of Chemical Industry, London, 1970, p. 315.
17 U. Costantino and A. Gasperoni, *J. Chromatogr.*, 51 (1970) 289.
18 M. J. Fuller, *J. Inorg. Nucl. Chem.*, 33 (1971) 559.
19 G. Alberti, U. Costantino and L. Zsinka, *J. Inorg. Nucl. Chem.*, 34 (1972) 3549.
20 A. Clearfield, A. M. Landis, A. S. Medina and J. M. Troup, *J. Inorg. Nucl. Chem.*, 35 (1973) 1099.
21 G. Alberti, S. Allulli, U. Costantino, P. Galli, M. A. Massucci and R. Platania, in J. A. Mikes (Editor), *IInd Symposium on Ion Exchange*, Vol. I, Magyar Kemikusok E., Budapest, 1969, p. 1.
22 G. Alberti, S. Allulli, U. Costantino, M. A. Massucci and E. Torracca, *Ion Exchange in the Process Industries*, Society of Chemical Industry, London, 1970, p. 318.
23 A. Clearfield, G. H. Nancollas and R. H. Blessing, in J. A. Marinsky and Y. Marcus (Editors), *Ion Exchange and Solvent Extraction*, Vol. 5, Marcel Dekker, New York, 1973, Ch. 1.
24 A. Clearfield and G. D. Smith, *Inorg. Chem.*, 8 (1969) 431.
25 A. Clearfield and W. L. Duax, *Acta Crystallogr.*, B25 (1969) 2658.
26 J. Albertsson, *Acta Chem. Scand.*, 20 (1966) 1689.
27 S. Ahrland, J. Albertsson, A. Alnas, S. Hemmingsson and L. Kulberg, *Acta Chem. Scand.*, 21 (1967) 195.
28 A. Ruvarac and V. Veselý, *J. Inorg. Nucl. Chem.*, 32 (1970) 3939.
29 G. Alberti, S. Allulli, U. Costantino, M. A. Massucci and M. Pelliccioni, *J. Inorg. Nucl. Chem.*, 35 (1973) 1347.

30 A. Clearfield, A. Oskarsson and C. Oskarsson, *Ion Exchange and Membranes*, 1 (1972) 91.
31 G. Alberti, S. Allulli, U. Costantino and M. A. Massucci, *J. Inorg. Nucl. Chem.*, in press.
32 S. E. Horsley and D. V. Nowell, *J. Appl. Chem. Biotechnol.*, 23 (1973) 215.
33 A. Clearfield and J. Troup, *J. Phys. Chem.*, 74 (1970) 1314.
34 E. Torracca, *J. Inorg. Nucl. Chem.*, 31 (1969) 1189.
35 G. Alberti, S. Allulli, U. Costantino, M. A. Massucci and N. Tomassini, *J. Inorg. Nucl. Chem.*, 36 (1974) 653.
36 A. Dyer, D. Leigh and F. T. Ocon, *J. Inorg. Nucl. Chem.*, 33 (1971) 3141.
37 S. E. Horsley and D. V. Nowell, *Thermal Analysis, Proc. 3rd ICTA, Davos*, Vol. 2, 1971, p. 611.
38 G. Alberti, S. Allulli, U. Costantino, M. A. Massucci and N. Tomassini, *J. Inorg. Nucl. Chem.*, 36 (1974) 660.
39 A. Clearfield, D. L. Duax, A. S. Medina, G. D. Smith and J. R. Thomas, *J. Phys. Chem.*, 73 (1969) 3424.
40 A. Clearfield, W. L. Duax, J. M. Garces and A. S. Medina, *J. Inorg. Nucl. Chem.*, 34 (1972) 329.
41 G. Alberti and U. Costantino, in preparation.
42 G. Alberti, unpublished results.
43 G. Alberti, U. Costantino and J. P. Gupta, *J. Inorg. Nucl. Chem.*, 36 (1974) 2103.
44 A. Clearfield and A. S. Medina, *J. Inorg. Nucl. Chem.*, 32 (1970) 277.
45 Y. Hasegawa and H. Aoki, *Bull. Chem. Soc. Jap.*, 46 (1973) 836.
46 G. Alberti, S. Allulli, U. Costantino and M. A. Massucci, *Gazz. Chim. Ital.*, 103 (1973) 819.
47 G. Alberti, S. Allulli, U. Costantino and M. A. Massucci, *J. Inorg. Nucl. Chem.*, 35 (1973) 1339.
48 G. Alberti and S. Allulli, *J. Chromatogr.*, 32 (1968) 379.
49 G. Alberti, S. Allulli and G. Cardini, *J. Chromatogr.*, 45 (1969) 298.
50 S. Allulli, A. La Ginestra and N. Tomassini, *J. Inorg. Nucl. Chem.*, in press.
51 R. M. Barrer and L. Hinds, *J. Chem. Soc.*, (1953) 1879.
52 G. Alberti, U. Costantino and J. S. Gill, in preparation.
53 G. Alberti, R. Bertrami, U. Costantino and J. P. Gupta, in preparation.
54 G. Alberti, U. Costantino and J. P. Gupta, *J. Inorg. Nucl. Chem.*, 36 (1974) 2109.
55 G. Alberti, M. G. Bernasconi and U. Costantino, in preparation.
56 A. Clearfield and G. D. Smith, *J. Inorg. Nucl. Chem.*, 30 (1968) 327.
57 G. Alberti, U. Costantino and M. Pelliccioni, *J. Inorg. Nucl. Chem.*, 35 (1973) 1327.
58 S. J. Harvie and G. H. Nancollas, *J. Inorg. Nucl. Chem.*, 32 (1970) 3923.
59 S. Allulli, A. La Ginestra, M. A. Massucci, M. Pelliccioni and N. Tomassini, *Inorg. Nucl. Chem. Lett.*, 10 (1974) 337.
60 A. Clearfield and J. M. Troup, *J. Phys. Chem.*, 74 (1970) 2578.
61 A. Dyer and F. T. Ocon, *J. Inorg. Nucl. Chem.*, 73 (1971) 315.
62 G. Alberti, R. Bertrami and U. Costantino, in preparation.
63 G. Alberti, U. Costantino and M. L. Luciani, in preparation.
64 G. Eisenman, *Biophys. J.*, 2 (1962) 259.
65 G. Alberti and U. Costantino, *J. Chromatogr.*, 50 (1970) 482.
66 G. Alberti *et al.*, work in progress.
67 G. Alberti, U. Costantino, M. L. Luciani, in preparation.
68 G. Alberti, M. A. Massucci and E. Torracca, *J. Chromatogr.*, 30 (1967) 579.
69 W. A. Chylley, *Ph.D. Thesis*, University of Wisconsin, Madison, Wisc., 1963.
70 S. Allulli, A. La Ginestra and M. A. Massucci, personal communication.